



# The process of combustion synthesis of WC–Co composites under the action of an electric field

Keqin Feng, Ji Xiong, Lan Sun\*, Hongyuan Fan, Xiang Zhou

School of Manufacturing Science and Engineering, Sichuan University, No. 24 Yihuan Road, Chengdu, Sichuan 610065, PR China

## ARTICLE INFO

### Article history:

Received 28 March 2010  
Received in revised form 14 May 2010  
Accepted 21 May 2010  
Available online 2 June 2010

### Keywords:

Composite materials  
Chemical synthesis  
Diffusion  
Scanning electron microscopy  
X-ray diffraction

## ABSTRACT

Composites of WC–Co have been synthesized and consolidated simultaneously at the ignition temperature of 794 °C by a field-assisted combustion synthesis method (EFACS), where the electric field was generated by a Gleeble thermal simulation instrument. Then, with the aid of high-temperature XRD results, the combustion synthesis process of an 88 wt% (W + C)–12 wt% Co system was studied according to quenching at different temperatures by turning off the electric field. A four-step model describing the process of combustion synthesis of WC–Co composites under an electric field, which is controlled by solid diffusion among the reactant atoms, is proposed. From the preheating period to the solid diffusion period, the solid diffusion among reactant atoms enhance with the increase of temperature. From the solid diffusion period to the combustion period, the  $2W_{(s)} + C_{(s)} = W_2C_{(s)}$  reaction may occurs at some interfaces between W and C atoms. During combustion period,  $2W_{(s)} + C_{(s)} = W_2C_{(s)}$  occurs firstly and follows the reaction of  $W_2C_{(s)} + C_{(s)} = 2WC_{(s)}$ . Co melts and then reacts to W,  $W_2C$  in order to form WC and  $Co_3W_3C$ , with that  $Co_3W_3C$  carbonizes to form WC and Co. After the combustion period, the remaining phases of  $W_2C$  and  $Co_3W_3C$  can be carbonized to form WC with the increase of temperature, and the morphology of tungsten carbide changes from spheroid to polyhedrons as the temperature rises.

© 2010 Elsevier B.V. All rights reserved.

## 1. Introduction

WC–Co composites which are used widely in tools for machining, cutting, drilling, and other applications are attractive for researchers because they are extremely hard, have an excellent wear resistance, as well as better toughness and strength than those of other hard materials [1,2]. WC–Co composites are normally prepared by a powder metallurgy route, which is a procedure consisting of a series of long-time processes, such as synthesis of WC powder, mixing with metal, granulation, pressing and sintering [3]. Moreover, the carbonization temperature of WC is as high as 1400–1600 °C [4], and a high sintering temperature and a long holding time are usually used by conventional sintering, which result in loss of the fine grain structure and the associated benefits of enhanced mechanical properties of the system. An alternative method that could synthesize and densify the WC–Co composites in one step at a lower reaction temperature and in a shorter time is the more energy-efficient combustion synthesis (CS) or self-propagating high-temperature synthesis (SHS). Combustion synthesis has been successfully used to produce a variety of refractory materials including ceramics, ceramic–metal composites, and intermetallic compounds [5,6]. However, it is well known that the

tungsten carbides have low adiabatic temperatures ( $T_{ad,Wc} = 1400$  K and  $T_{ad,W_2C} = 946$  K), which are considerably lower than the empirically established minimum of 1800 K for normal CS [7]. Especially, the adiabatic temperature of a W–C–Co system decreases with the increase of cobalt as binder. Consequently, such systems cannot be ignited without addition activation thanks to the relatively low heat of formation.

Recently, electric field-assisted combustion synthesis (EFACS) has been proven to be able to produce many kinds of high-quality materials due to the promoted diffusion among the reactant atoms, and thus it attracts more and more scientist's attention [8,9]. Electric field can serve as the additional energy source needed for activating and maintaining the combustion reactions that are otherwise difficult to occur or may react incompletely using unassisted combustion synthesis. As to our knowledge, no report has been found on electric field-assisted combustion synthesis of WC–Co composites except for Jiang et al. [7,10] and our research group [11]. Jiang uses an external ignition equipment (tungsten coil heating element) to quickly raise the system temperature in order to ignite the reactants in an EFACS process. The ignition source is turned off immediately after the reaction is initiated and an electric field is imposed simultaneously so that the reaction wave is able to propagate. In other words, the electric field only plays the roles of maintaining and controlling the process of combustion synthesis as a heating source. In our research, a much easier way is to use a high electric field as an ignition source so that the external

\* Corresponding author. Tel.: +86 28 85407310; fax: +86 28 85460940.  
E-mail address: [scutd@sina.com](mailto:scutd@sina.com) (L. Sun).

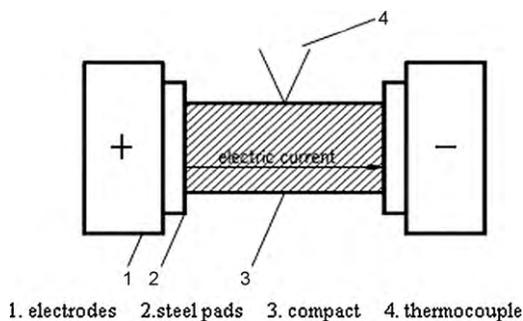


Fig. 1. Schematic representation of the Gleeble equipment.

ignition equipment can be omitted. In this method, the existence of a high electric current can not only maintain and control the process of combustion, but also significantly promote diffusion process among the reactant atoms and lower the ignition temperature of the reaction system. In this process, the whole sample combusts without wave propagation as in a thermal explosion mode, in which the ignition temperature is much lower than the synthesis temperature currently used in the normal methods [11,12].

This paper investigates the process of the combustion synthesis of an 88 wt% (W + C)–12 wt% Co system with  $T_{ad} = 823$  K under the action of an electric field, and proposes a model for the describing its behavior.

## 2. Experimental procedures

Powders of tungsten, cobalt (both of them with a 99% purity and an average grain size of  $3 \mu\text{m}$ ), and powders of graphite with a 98% purity and an average grain size of  $75 \mu\text{m}$ , were mixed thoroughly with a composition of 88 wt% (W + C)–12 wt% Co (W/C molar ratio of 1:1), and dry milled for 6 h. The mixed powders were compressed in a steel-mould to form a green compact with a diameter of 13.3 mm, a height of 7.8 mm, and a relative density of 73%. The green compact was then placed in a Gleeble thermal simulation instrument (Dynamic System Inc., USA) where it was heated and combusted to form a WC–Co composite under an electric field. Furthermore, the mixed powders were analyzed by high-temperature XRD before the quenching tests.

### 2.1. High-temperature XRD inspection of W–C–Co system

The mixed powders were put into a high-temperature XRD apparatus (Bruker, Cu  $K\alpha$ /50 kV/160 mA) and heated to different temperatures from low temperature to high temperature ( $450^\circ\text{C}$ ,  $650^\circ\text{C}$ ,  $850^\circ\text{C}$ ,  $1100^\circ\text{C}$ ,  $1250^\circ\text{C}$ ) orderly at a constant heating rate of  $4^\circ\text{C/s}$  in vacuum. When the temperature of mixed powders was steady, it was inspected by X-ray diffraction. After that, the mixed powders were heated to the next higher temperature and repeated the same procedure.

### 2.2. Combustion synthesis test

Fig. 1 shows the schematic of the experimental setup for the combustion synthesis. The green compact was sandwiched in between two steel pads that were in close contact with the two electrodes of the Gleeble thermal simulation instrument, which provided a high electric current through the sample. A thermocouple was placed on the surface of the sample to measure the sample temperature. In order to verify the uniformity of the sample temperature during the heating process, a separate experiment was performed in which the temperatures at different positions of the sample were measured simultaneously and compared. The maximum temperature difference between the surface and the centre of the sample was only  $3\text{--}5^\circ\text{C}$ . Therefore, only the surface temperature was measured in the rest of the experiments. Both of the actual temperature data and the axial shrinkage data of the compact during the experiment were recorded at a frequency of 20 Hz. Furthermore, in order to keep effective contact between the compact and Gleeble electrodes, a certain uniaxial low mechanical pressure was exerted on the compacts.

The combustion synthesis experiments are divided into two kinds, one kind is to investigate the characteristic of W–C–Co system combustion synthesis as shown in Section 2.2.1, in which the ignition temperature and the final synthesis product can be realized, but the microstructure evolution of the system at different stages cannot be known; whereas the other is to study the intermediate process of W–C–Co system combustion synthesis by quenching experiments at different temperatures, as shown in Section 2.2.2.

After the samples were cooled to room temperature, the phases of the synthesized products were analyzed by X-ray diffraction (XRD, D/Max-III A). The

microstructures of the sample cross-sections were examined by metaloscope and scanning electron microscope (SEM, JSE-5900LV) equipment with an energy dispersive spectrometer (EDS).

### 2.2.1. Investigation for the characteristic of W–C–Co system combustion synthesis

A green compact was firstly heated to  $200^\circ\text{C}$  at a preset heating rate of  $50^\circ\text{C/s}$  and held for 2 min in vacuum ( $<10^{-3}$  Pa), and then heated to  $1250^\circ\text{C}$  at the same heating rate and held for 6 min with the use of a high electric current (up to 12,300 A) passing through it. By analyzing the temperature and axial shrinkage profiles of the sample during the combustion synthesis process, the characteristic of W–C–Co system combustion synthesis could be obtained.

### 2.2.2. The quenching experiments of W–C–Co system combustion synthesis

The aim of the quenching experiments is to investigate the evolution process of W–C–Co system combustion synthesis at different stages. Based on these results of high-temperature XRD and the characteristic of W–C–Co system combustion synthesis, the quenching temperatures were in agreement to high-temperature XRD spectra experiment. The same set of samples were firstly heated to  $200^\circ\text{C}$  at a preset heating rate of  $50^\circ\text{C/s}$  via the electric current and held for 2 min in vacuum, and then heated with the same constant heating rate up to these target temperatures of  $450^\circ\text{C}$ ,  $650^\circ\text{C}$ ,  $850^\circ\text{C}$ ,  $1100^\circ\text{C}$ , and  $1250^\circ\text{C}$ , respectively. As soon as these temperatures were reached, switch off immediately the electric field. Thus, the microstructure evolution during the heating process of this system can be frozen in the quenched samples. By analyzing the microstructures and compositions of products at different temperatures, detailed information on the intermediate and phase transformation process during the combustion could be obtained.

## 3. Results and discussion

### 3.1. Combustion synthesis of WC–Co composites under an electric field

Fig. 2(a) shows the temperature and axial shrinkage profiles of the sample during the heating process. According to the characteristic of this temperature profile, the process can be described

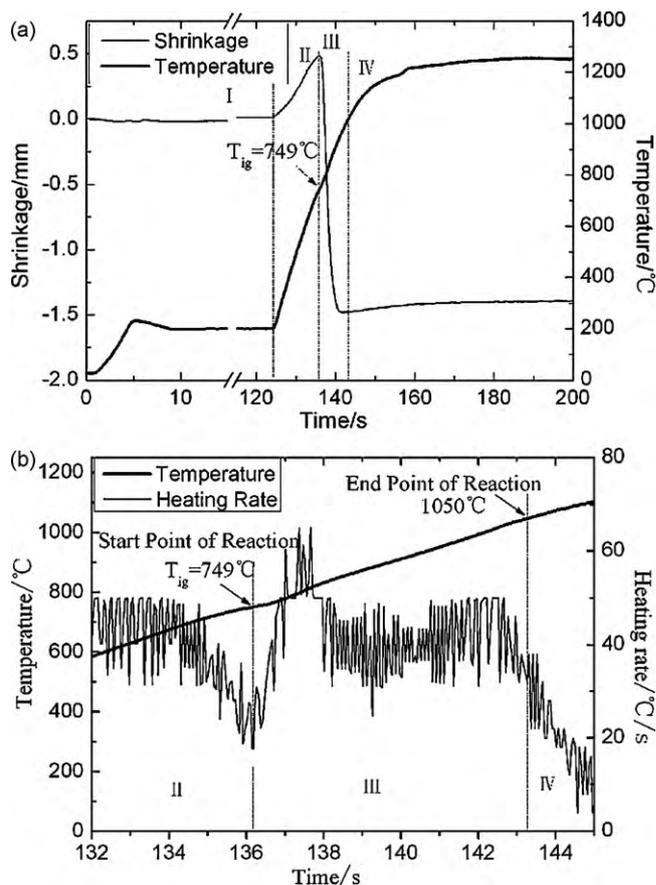


Fig. 2. (a) The temperature and axial shrinkage of the compact as a function of time; (b) the temperature and heating rate of the compacts as a function of time.

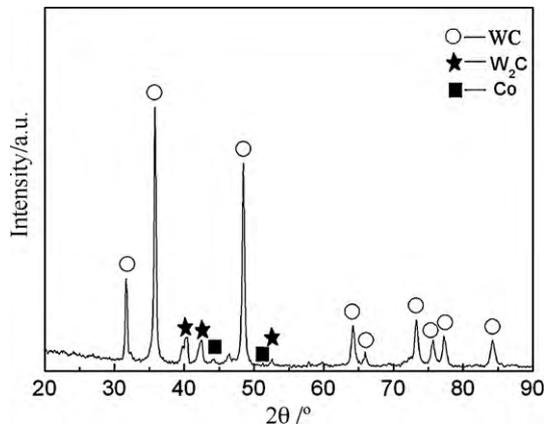


Fig. 3. XRD pattern of a final combustion synthesized product by EFACS.

as four periods: (I) preheating period (from the room temperature to the end of holding at 200 °C); (II) solid diffusion period (from the end of holding at 200 °C to the ignition temperature ( $T_{ig}$ )); (III) combustion period (from the ignition temperature to the end point of combustion); (IV) late-heating period (from the end of combustion to the end of heating process). The ignition temperature is defined as the onset temperature at the point where the temperature increases rapidly, representing the start of the synthesis reaction due to the onset of combustion and heat release from the system. The end point of combustion is defined as the point where the heating rate reduces to the same as that of the ignition temperature. The ignition delay time is defined as the time from the start of the heating process (from the room temperature) to the time when the system reaches ignition temperature [13]. By taking the derivative of the temperature with time, the actual heating rate profile was calculated as shown in Fig. 2(b), and the ignition temperature and ignition delay time were accurately measured. It is worth to mention that the actual heating rate of compact was lower than the preset heating rate except for the period of combustion, which due to the resistance from the compact. Therefore, correlation between system temperature and time is not always linear in the whole heating process. Close to the ignition point, the actual heating rate of compact decreased because the compacts need to absorb a large amount of energy in order to overcome the activation energy barrier of the combustion reaction.

In the preheating period (0–124 s), there is no obvious axial change of the sample. After the end of holding at 200 °C, an expansion of the sample is observed, this increases with the continuation of the heating process up to the ignition temperature. And Joule heat provided for the system can accelerate the solid diffusion among the reactant atoms, thus this stage is called solid diffusion period. When the system temperature reaches 749 °C, the energy input is high enough to ignite the system and thermal explosion takes place at this ignition temperature; the heating rate is higher than 50 °C/s because of the energy release from the exothermic reaction. Accompanying with the combustion of the system within 7 s, a very obvious axial shrinkage of sample occurs, which indicates massive liquid appears as a consequence of the local high temperature during the period of combustion synthesis. After the end of combustion (1050 °C), the temperature rises more slowly and the axial shrinkage almost stops.

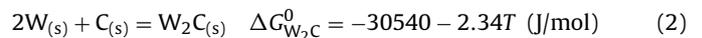
The XRD pattern of a final combustion synthesized product by EFACS is shown in Fig. 3, the product contains WC, a small amount of  $W_2C$  and Co, without the reactants W and C, which is consistent with the reported results [10,14]. As cited in Ref. [15], the C/W molar ratio of 1:1 resulted in an incompletely carburized phase  $WC_{1-x}$ . More carbon was needed to obtain the stoichiometric WC.

Therefore, the presence of  $W_2C$  along with WC in this product is unavoidable.

Fig. 4 shows the micrograph of the product. Fig. 4(a) indicates that a consolidation process occurs during the combustion synthesis of W–C–Co system. In fact, the relative density changes from 73% for green compact to 88.7% for the final compact. Furthermore, as shown in Fig. 4(b), many polygonal particles have been formed in the combustion product, which were identified as tungsten carbide by EDS. However, these sizes of particles are not quite uniform, which change from 1  $\mu\text{m}$  to 2.5  $\mu\text{m}$ .

Since the highest temperature of this heating process is less than the melting points of W (3407 °C), C (3527 °C), Co (1493 °C), WC (2800 °C) and  $W_2C$  (2785 °C), as well as the eutectic temperatures of the W–C system (2710 °C) and the melting point temperature of WC–Co system (1340 °C), then a solid–solid mechanism is the only likely process during the combustion synthesis of the carbide phase theoretically.

Fig. 5 and the following equations describe the free energy changes of the reactions of W–C system [16].



Both of the  $\Delta G$  values to form WC and  $W_2C$  are negative below 1700 K, but the  $\Delta G^\circ$  value for reaction (1) is smaller than that for reaction (2). It reveals thermodynamically that the two chemical reactions can take place below 1700 K, WC is more stable than  $W_2C$ , and  $W_2C$  can be carburized to form WC as much as possible. However, it is possible that  $\eta$  phase- $Co_3W_3C$  exists in the combustion product of W–C–Co system, and the reason why  $\eta$  phase form is attributed to the diffusion rate being much slower for W than for

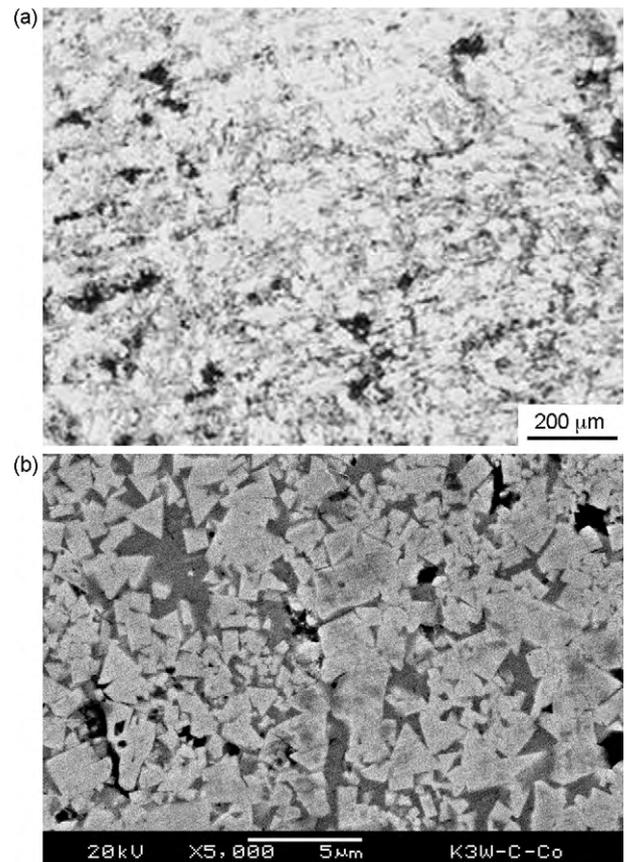


Fig. 4. The micrographs of combustion synthesized product: (a) metallograph; (b) SEM micrographs.

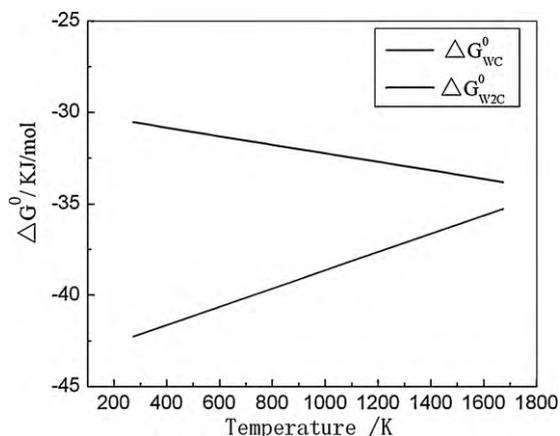


Fig. 5. The Gibbs free energy ( $\Delta G^0$ ) of WC and  $W_2C$  as a function of temperature.

C in Co [17]. But as the heating process continues, the  $\eta$  phase can decompose to form Co and WC with the diffusion of carbon [18,19].

### 3.2. Evolution of W–C–Co system in the heating process

In the process of the high-temperature XRD test, the sample was heated under a simplex thermal field by thermal radiation, which meant that electric field was not imposed on the samples directly. Fig. 6 shows the high-temperature XRD spectra of the W–C–Co system, there is no new phase formation except the reactants W, C and Co phases until the system was heated to 650 °C, no reactions occurs at this stage; but there is a small quantity of  $W_2C$  phase appearing in the heating period of 650–850 °C, as indicated the weak XRD peak of  $W_2C$ ; however, the WC phase was formed only at 1100 °C, and a large amount of WC and a small amount of  $W_2C$  were formed at 1250 °C. Especially the reactions to synthesize the tungsten carbides are incomplete; there is still a large amount of W remaining in the final product at 1250 °C.

Different from the high-temperature XRD test, an electric current passed through the samples directly in the EFACS, which provided Joule heating for the compacts by thermal conduction. And this co-effect of an electric field and self-generated thermal field enhanced mass transport of solid and liquid by electromigration, and markedly influenced the dynamics of reaction and the nature of product. A series of the XRD results and corresponding

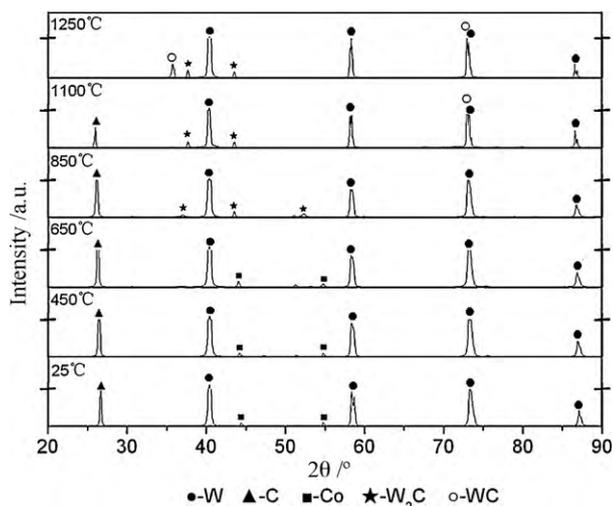


Fig. 6. High-temperature X-ray diffraction patterns of a W–C–Co system at various temperatures.

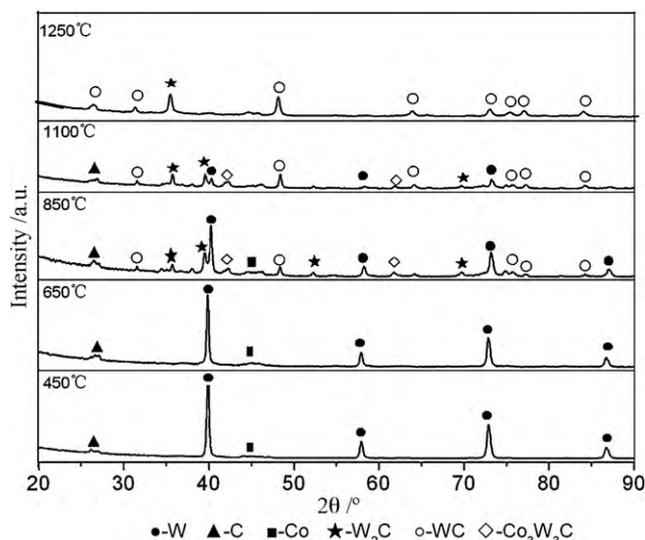


Fig. 7. X-ray diffraction patterns of stage products synthesized at different temperatures by EFACS.

SEM micrographs of the products synthesized at different heating temperatures which stand for different stages of EPACS, are shown in Figs. 7 and 8, respectively. As the same results as the high-temperature XRD test, the samples heated to 450 °C and 650 °C just only contain the reactant phases W, C and Co. Although no reaction occurs in the samples heated to 450 °C and 650 °C, the microstructures of the system have been changed to some degree. The diffusion phenomenon among reactant particles of the compact heated to 650 °C is more obvious than that of the compact heated to 450 °C. However, the reactant phases W, C and Co along with new phases  $W_2C$ , WC, and  $Co_3W_3C$  are present in the heating period of 650–850 °C. As mentioned above, the reactions of W–C–Co system occur at 749 °C, which is in the range of 650–850 °C. As the temperature increasing to 1100 °C, the diffraction peaks of WC phase intensify but those of W weaken; especially, all diffraction peaks of W and some diffraction peaks of  $W_2C$  have disappeared when the sample was heated to 1250 °C, which is different from the high-temperature XRD test. In other words, the phases of  $W_2C$  and  $Co_3W_3C$  can be carbonized to WC with the increase of temperature. The amount of polygonal particles, which are grey in the SEM micrographs and identified as tungsten carbide by EDS, increases as the temperature raise. And the average size of WC particles becomes bigger when the temperature increases. Compare with Fig. 4(b), the average size of WC particles in Fig. 8(e) is smaller because of the lack of 6 min holding time at 1250 °C. It is worth to mention that the pores in a compact decrease as the temperature rise, which accompanies with the densification of compact. Moreover, the reaction degree of W–C–Co system under an electric field is far more complete than that under a simplex thermal field.

### 3.3. Model of combustion synthesis process

Under this current activated combustion synthesis, the temperature and current are not independent parameters and thus the thermal effect of the current (Joule heat) cannot unambiguously be separated from the intrinsic role of the current. The influence of an electric field on diffusion can be attributed to one or more of the several intrinsic effects including electromigration, an increase in point defect concentration, and a reduction in mobility activation energy for diffusion [20]. An electric field has a pronounced effect on mass transport, which can be evaluated from the electromigration

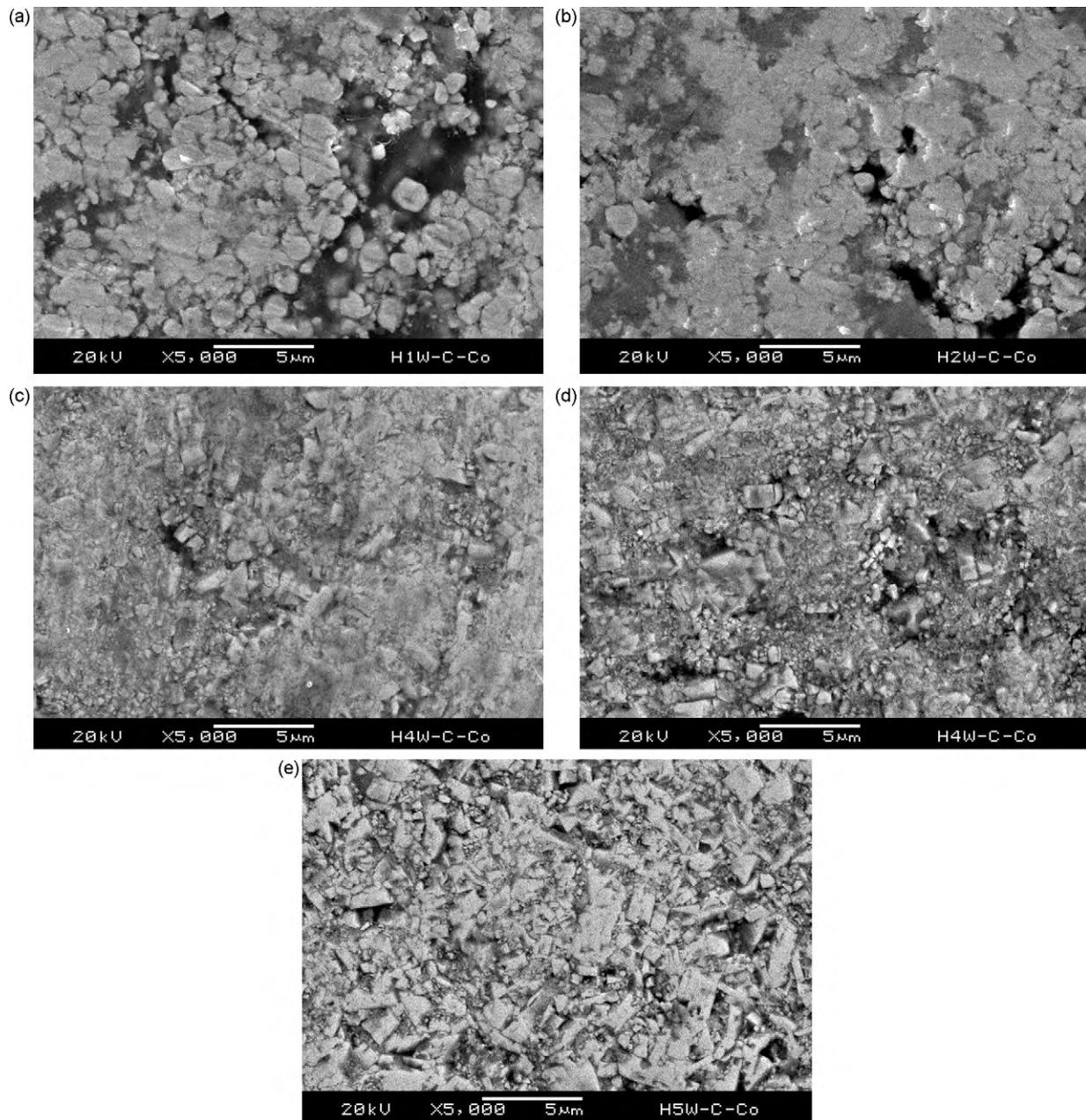


Fig. 8. SEM micrographs of samples synthesized at (a) 450 °C, (b) 650 °C, (c) 850 °C, (d) 1100 °C, and (e) 1250 °C.

theory [21]:

$$J_i = -\frac{D_i C_i}{RT} \left[ \frac{RT \partial \ln C_i}{\partial x} + Fz^* E \right] \quad (3)$$

where  $J_i$  is the flux of the diffusing into species,  $D_i$  is the diffusive coefficient of the species,  $C_i$  is the concentration of the species,  $F$  is Faraday's constant,  $z^*$  is the effective charge on the diffusing species,  $E$  is the field,  $R$  is the gas constant, and  $T$  is temperature.

The roles of electric field not only due to lowers the activations energy for diffusion and the activations energy for formation of the various phases in the system, but also increases the diffusive coefficient of the system. The effect of an electric field is dependent on its strength and the value of the effective charge of the diffusing atoms. In this EPACS experiment, the output electric current increases with the increase of the preset heating rate, and the preset heating rate is as high as 50 °C/s (corresponding to 12,300 A), which can signifi-

cantly enhance the solid diffusion of reactant atoms. As a result, the ignition temperature of the system can be significantly decreased.

On the basis of above experimental results, the process model of the combustion synthesis of a WC–Co composite under the action of an electric field is proposed, as described in Fig. 9.

- (1) From the preheating period to the solid diffusion period, due to the electric resistance and thermal resistance of compact decrease after holding at 200 °C, the current increases greatly and accelerates the solid diffusion among reactant atoms. Both C atoms and Co atoms diffuse into W particles, but the diffusion of C atoms into W atoms is faster than that of Co atoms into W atoms. However, the diffusive velocity and heating rate increase with the increase of temperature.
- (2) From the solid diffusion period to the combustion period, the  $2W_{(s)} + C_{(s)} = W_2C_{(s)}$  reaction may occur at some interfaces

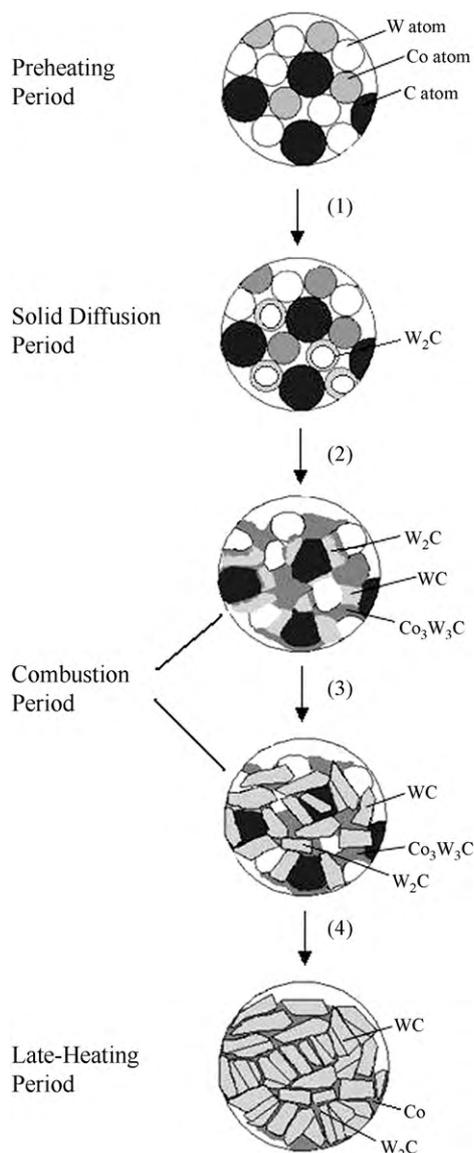
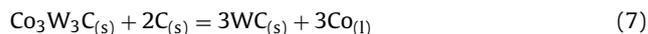
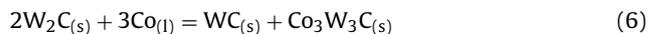
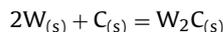


Fig. 9. The process of combustion synthesis of WC–Co composites.

between W and C atoms due to local high temperature in micro-zone of sample under the action of an electric field, in which C atoms diffuse into  $W_2C$  lattice by passing through the generated  $W_2C$  so as to continue this reaction. According to the “shell–core” model, the diffusion of C atoms is the rate-controlling step in this reaction.

- (3) When the system's energy obtained from an electric field is large enough to surmount the activation energy for reactions at  $749^\circ C$ , the system can be ignited in the form of thermal explosion. At the same time, although the temperature is lower than the melting temperature in W–C–Co system, the exothermic energy from the synthesis of tungsten carbide can induce local heating and cobalt melting. Once the liquid is formed, its further formation and spreading over the tungsten carbide particles are fast, due to surface energy. As a result, a large amount of liquid phase is formed, this can be evidenced by the appearance of an obvious axial shrinkage in the sample at the ignition temperature. And the melting Co can promote solid diffusion of the system as a consequence of the increase of interconnection between reactant particles. During the combustion period, the process of synthesis WC is shown as follow, which is consonant

with the previous report [22].



The reaction between W and C to form  $W_2C$  occurs firstly in the initial stage, and follows reaction (4). And then Co melts, reacts to W,  $W_2C$  and change to WC and  $Co_3W_3C$ . Finally,  $Co_3W_3C$  carbonize with the diffusion of carbon to form WC and Co, which means  $Co_3W_3C$  is a non-equilibrium transition phase of the non-equilibrium process-CS. However, it is difficult for W–C–Co system to react completely because of the short time of combustion period (7 s). Therefore, there are a few remaining phases of  $W_2C$  and  $Co_3W_3C$  in the sample at the end of combustion period.

- (4) After the combustion period, the remaining phases of  $W_2C$  and  $Co_3W_3C$  can be carbonized to WC with the increase of temperature. Finally,  $Co_3W_3C$  can be carbonized to WC completely whereas  $W_2C$  cannot. Nevertheless, there is no or just little liquid phase in the compact because there are no more obvious exothermic reactions providing the high energy needed. As the temperature rises, the morphology of tungsten carbide changes from spheroid to polyhedrons with distinguishing edges and corners because of the effect of Co [23], and Co spreads around WC grains to form WC–Co composites. The WC particles can be continuously formed by nucleation and crystal growth; the synthesized products consist of a large amount of WC particles and a small amount of  $W_2C$ .

The whole four-step synthesis process is controlled by solid diffusion among the reactant atoms. Since the electric field with high current can promote the solid diffusion at a lower temperature, the ignition temperature can be lowered greatly.

#### 4. Conclusions

Due to the co-effect of electric and thermal field imposed on W–C–Co system, the combustion synthesis reaction of the system occurs at  $749^\circ C$  in synchronism with the shrinkage of the compact under an electric field, and the synthesized products contain WC, a small amount of  $W_2C$  and Co. In other words, the simultaneous synthesis and densification of WC–Co composites is accomplished at lower temperature by electric field induction combustion synthesis.

The process of combustion synthesis of the WC–Co composites under the action of an electric field can be described as a four-step process: (I) from the preheating period to the solid diffusion period, the solid diffusion among reactant atoms enhance with the increase of temperature; (II) from the solid diffusion period to the combustion period, the exothermic reaction  $2W_{(s)} + C_{(s)} = W_2C_{(s)}$  reaction may occur in some interfaces; (III) during the combustion period, the  $2W_{(s)} + C_{(s)} = W_2C_{(s)}$  reaction occurs firstly in the initial stage, and follows the reaction of  $W_2C_{(s)} + C_{(s)} = 2WC_{(s)}$ . The exothermic energy released from the two reactions can induce local heating and cobalt melting. And then melting Co react to W,  $W_2C$ , and change to WC and  $Co_3W_3C$ . Finally,  $Co_3W_3C$  carbonize with the diffusion of carbon to form WC and Co; (IV) after the combustion period, the remaining phases of  $W_2C$  and  $Co_3W_3C$  can be carbonized to WC with the increase of temperature. There is no or just little liquid phase in the compact. As the temperature rises, Co spreads

around WC grains to form WC–Co composites, and the morphology of tungsten carbide changes from spheroid to polyhedrons with distinguishing edges and corners. The synthesized products consist of a large amount of WC particles and a small amount of  $W_2C$ . However, the whole four-step synthesis process is controlled by solid diffusion among the reactant atoms.

### Acknowledgements

This work was supported by the National Nature Science Foundation of China (No. 50404014) and China Postdoctoral Science Foundation (No. 20060390177). The authors would like to thank Mrs. Hui Wang in Analytical & Testing Center at Sichuan University for assistance in the experiments.

### References

- [1] R. Taegong, H.Y. Sohn, *Metall. Mater. Trans. B* 39 (2008) 1–6.
- [2] S. Lay, M. Loubradou, P. Daonnadieu, *Adv. Eng. Mater.* 6 (2004) 811–814.
- [3] F.P. Medeiros, S.A. De Oliverira, C.P. De Souza, *Mater. Sci. Eng. A* 315 (2001) 58–62.
- [4] M.F. Zawrah, *Ceram. Int.* 33 (2007) 155–161.
- [5] M.S. Songa, B. Huanga, M.X. Zhanga, *Int. J. Refract. Met. Hard Mater.* 27 (2009) 584–589.
- [6] Z.A. Munir, U. Anselmi-Tamburini, *Mater. Sci. Rep.* 3 (1989) 277–283.
- [7] G.J. Jiang, H.R. Zhuang, W.L. Li, *Scripta Mater.* 50 (2004) 1181–1185.
- [8] R. Orru, A. Cincotti, Z.A. Munir, *Chem. Eng. Sci.* 56 (2001) 683–690.
- [9] Z.A. Munir, *Mater. Sci. Eng. A* 287 (2000) 125–137.
- [10] G.J. Jiang, H.R. Zhuang, W.L. Li, *Combust. Flame* 135 (2003) 113–121.
- [11] J. Liu, Y. Yang, K.Q. Feng, *J. Alloys Compd.* 476 (2009) 207–212.
- [12] K.Q. Feng, M. Hong, *Int. J. Refract. Met. Hard Mater.* 27 (2009) 852–857.
- [13] V.V. Barzykin, *Pure Appl. Chem.* 64 (1992) 909–913.
- [14] M. Christensen, G. Wahnstr., *Acta Mater.* 52 (2004) 2199–2207.
- [15] A.P. Hagen, *Formation of Bonds to C, Si, Ge, Sn Pb (Part 4)*, first ed., VCH Publishers, New York, 1990.
- [16] D.L. Ye, *Utility Inorganic Thermodynamic Data Handbook*, first ed., Metallurgical Industry Press, Beijing, 1981.
- [17] O. Lavergne, F. Robaut, F. Hodaj, *Acta Mater.* 50 (2002) 1683–1692.
- [18] V. Ramnath, N. Jarayaman, *Mater. Sci. Technol.* 5 (1989) 382–388.
- [19] M.E. Vinayo, F. Kassabji, J. Guyonnet, *Sci. Technol. A* 3 (1985) 2483–2489.
- [20] Z.A. Munir, U. Anselmi-Tamburini, *J. Mater. Sci.* 41 (2006) 763–777.
- [21] H.B. Huntington, *Diffusion in Solids*, first ed., Academic Press, New York, 1975.
- [22] G.J. Jiang, H.R. Zhuang, W.L. Li, *J. Alloys Compd.* 387 (2005) 90–96.
- [23] Z.X. Ma, L.Y. Fu, *Cement. Carbide* 18 (2001) 4–7.